Pergamon

PII: S0277-5387(97)00073-9

Polyhedron Vol. 16, No. 19, pp. 3267–3271, 1997

0277-5387/97 $17.00+0.00

One-dimensional polymeric bicinate manganese complex

Ziming Sun, Peter K. Gantzel and David N. Hendrickson*

Department of Chemistry-0358, University of California at San Diego, La Jolla, CA 92093-0358, U.S.A.

(Received 9 January 1997)

Abstract—The synthesis, X-ray structure and magnetochemical properties of the one-dimensional polymeric bicinate (bic^-) manganese complex $\{[Mn(bic)Cl]_2 \cdot 2(H_2O)\}_n$ are reported. Each manganese ion has distorted octahedral coordination geometry. Bicine is a pentadentate ligand using one nitrogen, and four oxygen atoms to coordinate to the Mn^{II} ion. The two hydroxyl groups are not deprotonated and the carboxylate moiety of the bic^- ligand ion is a bridge leading to a one-dimensional chain. The water molecules are not coordinated to the Mn^{II} ions, but are involved in hydrogen-bonding interactions with the chain. Only weak pairwise antiferromagnetic exchange interactions ($J = -0.30\ cm^{-1}$) are found within the chain complex due to the carboxylate bridges. © 1997 Elsevier Science Ltd

Keywords: bicine; manganese; magnetic exchange; one-dimensional; polymer.

N,N-bis(2-hydroxyethylglycine)(bicine) is a widely used buffer substance in biochemical studies [1,2]. As with its parent compound glycine, and related compound *N*-(2)-hydroxyethyl)imminodiacetic acid (heidi) [3], bicine forms metal complexes. The stability constants of many transition metal complexes of bicinate have been determined and it has been found that the $[M(bic)]^+$ species (bic^- = bicinate) is always the predominate species in solution for divalent transition metal ions [4,5]. Even though metal complexes of bicinate have been studied for years, only complexes with copper ions have been structurally characterized [6–9]. In those structural studies it was found that bicine is a versatile ligand and functions either as a tetradentate ligand to form mononuclear metal complexes [6,7] or as a pentadentate ligand to form polymeric chain complexes [8].

Our interest in bicine as a ligand is twofold. First, its versatile coordination capacity leads to polymeric chain complexes which could support magnetic exchange interactions between metal ions. In addition, as with the ligand heidi, the ethanol hydroxyl groups of bicine could be deprotonated to form transition metal clusters that exhibit interesting properties as magnetic molecules. In other words, we are exploring the possibility of using bicine as a ligand to build molecular-based magnets. Here we report the synthesis, the X-ray structure, infrared spectrum and magnetic properties for the one dimensional polymeric Mn^{II} complex, $\{[Mn(bic)Cl]_2 \cdot 2(H_2O)\}_n$ (**1**).

EXPERIMENTAL

Instrumentation and materials

The ambient-temperature infrared spectrum was obtained on a Mattson 2020 Galaxy Series FTIR spectrophotometer. Variable-temperature magnetic susceptibility data were collected for a polycrystalline sample of complex **1** on a Quantum Design MPMS5 SQUID susceptometer equipped with a 55 kG magnet and operating in the range of 1.8–400 K. Diamagnetic correlations were estimated using Pascal's constants and were subtracted from the experimental molar susceptibility to obtain the paramagnetic molar susceptibilities [10]. Solvents and reagents were used as purchased.

Synthesis

$MnCl_2 \cdot 6H_2O$ (2.00 g, 10.1 mmol) and bicine (0.54 g, 3.33 mmol) were dissolved in 80 cm^3 methanol. A

* Author to whom correspondence should be addressed.

4.0 cm^3 25% methanolic solution of $[(CH_3)_4N]OH$ (10.0 mmol) was added dropwise. The color of the solution gradually changed from colorless to dark brown. X-ray quality crystals were obtained by slow evaporation over several days. Found: C, 26.2; H, 5.2; N, 5.1; Mn, 20.2; Calc. for $\{[Mn(bic)Cl]_2 \cdot 2(H_2O)\}_n$ (**1**): C, 26.6; H, 5.2; N, 5.2; Mn, 20.3%. The yield was 68.0% based on bicine.

X-ray crystallography

Data were collected at 299 K on a Siemens R3m/v four circle diffractometer, employing Mo-K_α ($\lambda = 0.71073$ Å) radiation with a graphite crystal monochromator. Data were measured by using Wyckolf omega scans. Crystallographic data and other pertinent information are given in Table 1. Selected bond distances and angles are listed in Table 2. Lorentz and polarization corrections were applied and direct methods (SHELXTL PC) revealed the structure. The structure was refined in the space group $P2_1/n$ using anisotropic thermal parameters for all non-hydrogen atoms and isotropic ones for the hydrogen atoms. The positional parameters of all hydrogen atoms were included in the least-squares refinement cycles. The discrepancy indices $R = (\Sigma||F_o| - |F_c||)/\Sigma|F_o|$ and $R_w = [\Sigma w(|F_o| - |F_c|)^2/\Sigma w|F_o|^2]^{1/2}$ are listed in Table 1.

RESULTS AND DISCUSSION

Compound preparation

The goal in this research was to prepare a polynuclear manganese complex that incorporated Mn^{III} ions and the bicinate anion. In order to prepare a high nuclearity Mn^{III} complex, a *basic* methanol solution containing Mn^{II} and bicine was allowed to react in the air. It is clear that some of the Mn^{II} was oxidized, for the color of the solution changed from colorless to dark brown. Two products were isolated: colorless crystals that analyzed as $\{[Mn(bic)Cl]_2 \cdot 2(H_2O)\}_n$ (**1**) and a dark brown solid. Efforts are continuing to characterize the brown solid. In the following is given a characterization of the colorless crystals of complex **1**.

X-ray structure

The polymeric structure of complex **1** is comprised of a $[Mn(bic)Cl]_2$ repeating unit with two hydrogen bonded H_2O molecules. The one-dimensional structure is shown in Fig. 1 together with the atom-numbering scheme. The carboxylate moiety of the bicinate ligand acts as a bis(monodentate) bridging ligand that is bonded on each side to Mn^{II} ions *via* carboxylate oxygen atoms in *syn*- and *anti*- conformations, yield-

Table 1. Crystallographic data

Formula	$C_6H_{14}ClMnNO_5$
Formula weight	270.6
Temperature (K)	297
Wavelength (Å)	0.71073
Crystal system	Monoclinic
Space group	$P2_1/n$
a (Å)	10.382(2)
b (Å)	9.471(2)
c (Å)	10.843(2)
β (°)	94.54(3)
V (Å^3)	1062.9(9)
Z	40
Density ρ (mg m^{-3})	1.691
Range of 2θ (°)	3–55
Absorption coefficient (mm^{-1})	3.456
$F(000)$	1488
Crystal size (mm)	$0.4 \times 0.4 \times 1.0$
Index range	$0 \leqslant h \leqslant 13$, $-12 \leqslant k \leqslant 0$, $-14 \leqslant l \leqslant 14$
No. unique data	2450
Data with $F_o^2 > 4\alpha(F_o^2)$	2092
Refinement method	Full matrix least-squares on F
R	0.028
R_w	0.0345
Largest diff. peak (e Å^{-3})	0.28
and hole (e Å^{-3})	−0.47

Table 2. Selected bond distances (Å) and angles (°)

Mn(1)—Cl(1)	2.509(1)	O(4)—Mn(1A)	2.126(2)
Mn(1)—O(1)	2.217(2)	C(6)—O(3)	1.253(2)
Mn(1)—O(2)	2.236(2)	C(6)—O(4)	1.270(2)
Mn(1)—O(3)	2.234(2)	O(5A)—H···O(4)	2.785
Mn(1)—O(4A)	2.126(2)	O(1)—H···O(5)	2.696
O(1)—Mn(1)—O(2)	96.7(1)	Cl(1)—Mn(1)—O(1)	85.4(1)
O(1)—Mn(1)—O(3)	141.4(1)	Cl(1)—Mn(1)—O(2)	177.6(1)
O(1)—Mn(1)—N(1)	74.7(1)	Cl(1)—Mn(1)—O(3)	84.6(1)
O(1)—Mn(1)—O(4A)	119.4(1)	Cl(1)—Mn(1)—O(4A)	92.5(1)
O(2)—Mn(1)—O(3)	93.0(1)	Cl(1)—Mn(1)—N(1)	105.1(1)
O(2)—Mn(1)—N(1)	74.4(1)	O(3)—C(6)—O(4)	123.5(2)
O(3)—Mn(1)—N(1)	72.1(1)	O(5A)—H···O(4)	171.1
O(3)—Mn(1)—O(4A)	98.2(1)	O(1)—H···O(5)	165.5
N(1)—Mn(1)—O(4A)	158.7(1)		

ing a chain that runs parallel to the *b* axis as depicted in Fig. 2. Within the chain the dimeric units are arranged head to tail, forming a *zig-zag* infinite chain. The water molecules are hydrogen bonded to two dimeric units and help to constrain the *zig-zag* chain. Each water molecule forms two strong intra-chain hydrogen bonds: the distances and angles of the O(5A)—H···O(4) and O(1)—H···O(5) units are 2.785 Å, 2.696 Å, 171.1°, and 165.5°, respectively. There are two anti-parallel chains running through each unit cell. The intra-chain distance and the inter-chain distance between two successive Mn^{II} ions are 4.987 Å and 7.204 Å, respectively.

Each Mn^{II} ion has a distorted octahedral coordination comprised of two hydroxy–oxygen atoms O(1) and O(2), one carboxylate oxygen atom O(3), one nitrogen atom N(1), one chlorine atom Cl(1) and another oxygen atom O(4A) from a second bicinate ligand. The Mn—N bond length (2.350 Å) is significantly longer than the Mn—O bond distances with carboxylate and hydroxyl oxygen atoms that are about 2.20 Å. This is different from what was found [6–9] in the bicinate copper complexes. For all copper complexes, at least one Cu—O bond (hydroxyl oxygen) is longer than Cu—N bond. This difference is likely the result of different coordination geometries. In the case of Mn^{II}, since it is six-coordinate this requires the five-membered chelate arms to be distorted from the conformation observed in the five-coordinate Cu^{II} complexes. Of course, the chloride ligand in the Mn^{II} complex contributes to twist the three five-membered rings, and the sterics of the Cl^- ligand could explain the long Mn—Cl bond (2.508 Å) [11]. There are small bond length differences for the two hydroxyl–oxygen atoms coordinated to the Mn^{II} ion (2.214 and 2.234 Å for Mn(1)—O(1), Mn(1)—O(2), respectively) and the two carboxylate oxygen atoms (2.229 and 2.120 Å for Mn(1)—O(3), Mn(1A)—O(4), respectively). The origin of these differences could be the intramolecular hydrogen

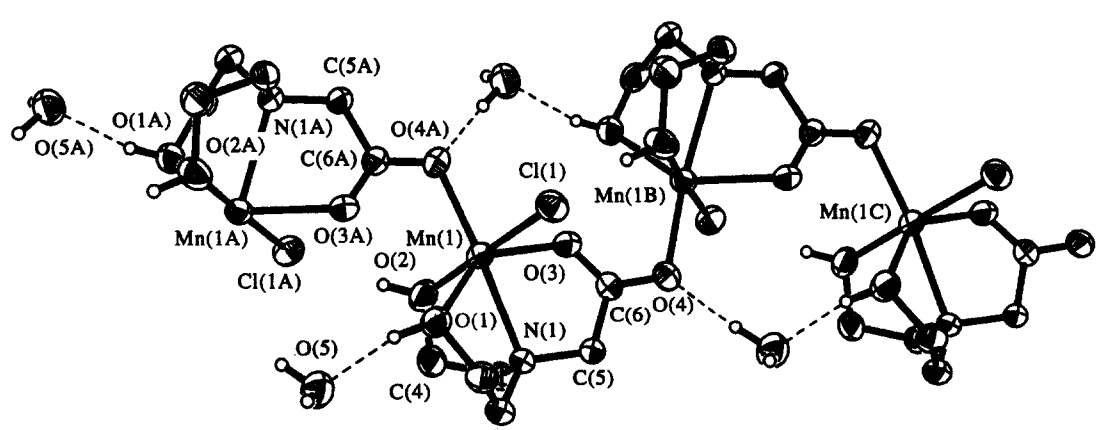

Fig. 1. X-ray structural representation of the linear chain in $\{[Mn(bic)Cl]_2 \cdot 2(H_2O)\}_n$ (complex **1**). Atoms are represented by their 50% probability ellipsoids. Hydrogen atoms on carbon atoms are omitted for clarity. Hydrogen-bonding contacts between H_2O molecules and oxygen atoms of the bic^- ligand are indicated by dashed lines.

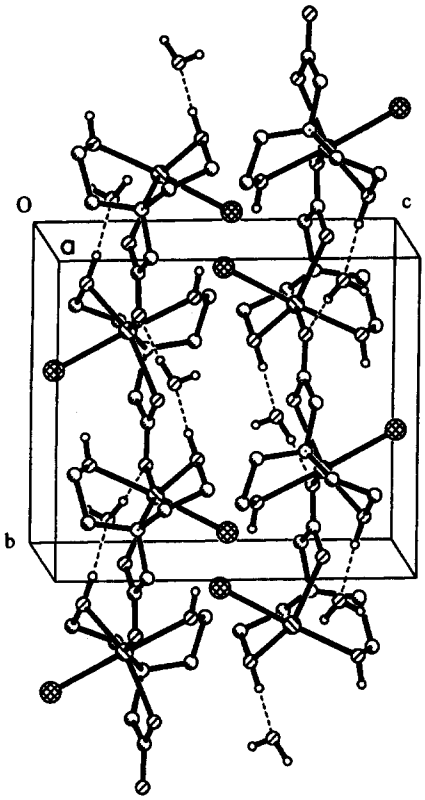

Fig. 2. Drawing showing the unit cell arrangements in $\{[Mn(bic)Cl]_2 \cdot 2(H_2O)\}_n$ (complex **1**).

bonds. Both O(1) and O(4) form strong hydrogen bonds with a water molecule. The formation of a hydrogen bond reduces the strength of the O—H bond in the hydroxyl group and this increases the interaction of Mn^{II} with either O(1) or O(4).

Large deviations from idealized octahedral geometry are found at the Mn^{II} center [74.6(1), 74.8(1) and 72.1(1)° for Cl(1)—Mn(1)—N(1), O(1)—Mn(1)—N(1) and O(3)—Mn(1)—N(1) respectively]. The best equatorial plane is defined by atoms O(1), O(2), O(3), Cl(1) where the manganese ion is 0.390 Å out of this plane toward the O(4A) atom that comes from another bicinate carboxylate group. This could be another way to explain the two different bond lengths for the carboxylate oxygen with Mn^{II} [i.e., the bond Mn(1A)—O(4) is shorter than the Mn(1)—O(3) bond]. The atom O(4) is on the apical site of the distorted octahedral coordination sphere and is less affected by repulsion from these oxygen atoms and the chlorine atom. This same effect has been reported [8] for the copper complexes. It has been found that ethyl hydroxyl group in the ligand heidi could be deprotonated and the oxygen could serve as a μ_3-oxo bridge which then results in a cluster [3]. In the case of complex **1**, the most remarkable structural feature is the pentadentate coordination of the bicinate ligand that supports a one-dimensional polymer.

Infrared spectroscopy

Three strong broad bands are found in the KBr-pellet IR spectrum for complex **1** at energies about 3000 cm^{-1}; they are found at 3525, 3362, and 3260 cm^{-1}. Based on the results [7] from studying [Cu(bic)Cl], in which the 3025 cm^{-1} band disappears upon deuteration, these bands are assigned to the OH stretching vibration for the bic^- ligand. The O(1)H stretching vibration should probably have the lowest frequency due to its hydrogen bond that decreases the electron density on the oxygen atom. The O(2)H stretching vibration would have a higher frequency because there is no hydrogen bond involved. All of the OH stretching vibrations are shifted to higher frequencies than those seen for the copper complexes, which could be interpreted to mean that the bond strength of Mn—O(hydroxyl) is not as strong as the metal—OH bonds in copper complexes. The higher frequency band seen for complex **1** at 3525 cm^{-1} should be from the H_2O vibration.

The bands at 1572 and 1412 cm^{-1} are assigned to the COO^- antisymmetric and symmetric stretching vibrations, respectively. They have almost the same energies as in the copper complexes [8].

Magnetochemistry of complex **1**

Variable-temperature dc magnetic susceptibility data were collected for a powder sample in a 10 kG field. A plot of the effective magnetic moment (μ_{eff}) per molecule or unit in the temperature range 2.0–320 K is shown in Fig. 3. A weak antiferromagnetic exchange interaction between Mn^{II} centers is evident. The effective magnetic moment per unit decreases slightly from 5.88 μ_B at 320 K to 5.75 μ_B at 80.0 K and then more rapidly to 2.32 μ_B at 2.00 K.

The data were analyzed assuming isotropic Hei-

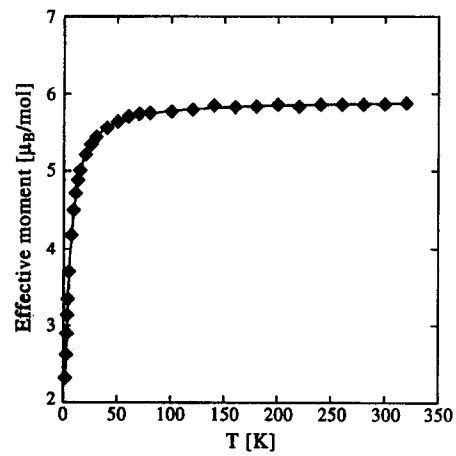

Fig. 3. Plot of the effective magnetic moment *vs* temperature for a powder sample of $\{[Mn(bic)Cl]_2 \cdot 2(H_2O)\}_n$ (complex **1**). Data were collected in a 10.0 kG field. The solid line represents the best fit of the data to eq. (2).

senberg pairwise interactions between Mn^{II} ions in a linear chain. The spin Hamiltonian is given in eq. (1). Wagner and Friedberg [12] derived the equation for the magnetic susceptibility for a linear chain with $S = 5/2$ in eq. (2), where $U = \coth(K - 1/K)$ and $K = 2\mathbf{J}S(S+1)/kT$.

$$H = -2\mathbf{J}\sum_{i=1}^{n} S_i \cdot S_{i-1} \quad (1)$$

$$\chi_M = \{Ng^2\mu_B^2 S(S+1)/3kT\}\{(1+U)/(1-U)\} \quad (2)$$

The parameters are **J** for the magnetic exchange interaction and an isotropic g value. The solid curve in Fig. 3 represents the least-squares fit of the data to eq. (2) to give the parameters $\mathbf{J} = -0.30\ cm^{-1}$ and $g = 1.98$. It can be seen that the agreement between the theory and experimental data is quite satisfactory.

Much effort has been spent to synthesize and characterize Mn^{II} linear chain complexes [12–20]. Three types of bridging ligands have been found which support weak antiferromagnetic interactions; carboxylate, phosphinate and chloride ions. The magnetic exchange parameter **J** varies from $-9.3\ cm^{-1}$ for the chloro bridge to $-0.2\ cm^{-1}$ for the carboxylate and phosphinate bridges [12–20]. The **J** value for complex **1** is within this range. The relatively weak antiferromagnetic interaction in complex **1** reflects the more extended bridge of the carboxylate unit in the bicinate ligand.

For the only two bicinate copper polymeric chain complexes that have been reported [8,9] negligible magnetic exchange interactions have bene found. [Cu(bic)(SCN)] has an SCN^- bridge (Cu···Cu, 6.29 Å) that is 1.30 Å longer than the bridge in complex **1** [9]. This could explain the very weak magnetic interaction between neighboring Cu^{II} ions in $[Cu(bic)(SCN)^-]_n$. For $[Cu(bic)]ClO_4 \cdot H_2O$ the Cu···Cu distance (5.030 Å) is very close to the distance in complex **1**. The Cu^{II} ions in this ClO_4^- complex have five-coordinate trigonal bipyramidal coordination geometries. There is no evidence of $Cu^{II}\cdots Cu^{II}$ magnetic exchange interactions in $[Cu(bic)]ClO_4 \cdot H_2O$.

Acknowledgement—This work was supported by National Science Foundation grant CHE-9420322 (D.N.H.).

REFERENCES

1. Sigel, H., *Coord. Chem. Rev.*, 1993, **122,** 227.
2. Krishnamoorthy, C. R. and Nakon, R., *J. Coord. Chem.*, 1991, **23,** 233.
3. (a) Powell, A. K., Heath, S. L., Gatteschi, D., Pardi, L., Sessoli, R., Spina, G., Del Giallo, F. and Pieralli, F., *J. Am. Chem. Soc.*, 1995, **117,** 2491; (b) Heath, S. L. and Powell, A. K., *Angew. Chem. Int. Ed. Engl.*, 1992, **31,** 191.
4. Ji, L.-N., Corfu, N. A. and Sigel, H., *Inorg. Chim. Acta.*, 1993, **206,** 215.
5. Curfu, N. A., Song, B. and Ji, L.-N., *Inorg. Chim. Acta.*, 1992, **192,** 243.
6. Yamaguchi, H., Nagase, M., Yukawa, Y., Inomata, Y. and Takeuchi, T., *Bull. Chem. Soc. Jpn.*, 1988, **61,** 2763.
7. Yamaguchi, H., Inomata, Y. and Takeuchi, T., *Inorg. Chim. Acta.*, 1991, **181,** 31.
8. Yamaguchi, H., Inomata, Y. and Takeuchi, T., *Inorg. Chim. Acta.*, 1989, **161,** 217.
9. Yamaguchi, H., Inomata, Y. and Takeuchi, T., *Inorg. Chim. Acta.*, 1990, **172,** 105.
10. Boudreaux, E. A. and Mulay, L. N., eds, *Theory and Applications of Molecular Paramagnetism*, J. Wiley & Sons, New York, 1976.
11. Goldberg, D. P., Caneschi, A., Delfs, C. D., Sessoli, R. and Lippard, S. J., *J. Am. Chem. Soc.*, 1995, **117,** 5789.
12. Wagner, G. R. and Friedberg, S. A., *Phys. Lett.*, 1964, **9,** 11.
13. Dingel, R., Lines, M. E. and Holt, S. L., *Phys. Rev.*, 1969, **187,** 643.
14. Weng, W., Bartik, T. and Gladysz, J. A., *Angew. Chem. Int. Ed. Engl.*, 1994, **33,** 2199.
15. Cicha, W. V., Hayes, J. S., Oliver, K. W., Rettig, S. J., Thompson, R. C. and Trotter, J., *Can. J. Chem.*, 1985, **63,** 1055.
16. Du, J.-L., Rettig, S. J., Thompson, R. C. and Trotter, J., *Can. J. Chem.*, 1992, **70,** 73217.
17. Bino, P. B. A., Du, J.-L., Lo, L. S.-M. and Thompson, R. C., *Inorg. Chim. Acta.*, 1990, **170,** 45.
18. Borras-Alamenar, J. J., Burriel, R., Coronado, E., Gatteschi, D., Gomez-Garcia, C. J. and Zanchini, C., *Inorg. Chem.*, 1991, **30,** 947.
19. Borras-Alamenar, J. J., Coronado, E., Gomez-Garcia, C. J., Gatteschi, D. and Zanchini, C., *J. Appl. Phys.*, 1990, **67,** 6006.
20. Biagini-Cingi, M., Manotti-Lanfredi, A. M., Ugozzoli, F., Haasnoot, J. G. and Reedijk, J., *Gazz. Chim. Ital.*, 1994, **124,** 509.